



Published in final edited form as:

*Biochem Biophys Res Commun.* 2015 August 21; 464(2): 554–560. doi:10.1016/j.bbrc.2015.07.005.

## The actin family protein ARP6 contributes to the structure and the function of the nucleolus

Hiroshi Kitamura<sup>a,1</sup>, Haruka Matsumori<sup>b,1</sup>, Alzbeta Kalendova<sup>c</sup>, Pavel Hozak<sup>c</sup>, Ilya G. Goldberg<sup>d</sup>, Mitsuyoshi Nakao<sup>b,e</sup>, Noriko Saitoh<sup>b</sup>, and Masahiko Harata<sup>a,\*</sup>

<sup>a</sup>Laboratory of Molecular Biology, Graduate School of Agricultural Science, Tohoku University, Tsutsumidori-Amamiyamachi 1-1, Aoka-ku, Sendai 981-8555, Japan

<sup>b</sup>Department of Medical Cell Biology, Institute of Molecular Embryology and Genetics, Kumamoto University, 2-2-1 Honjo, Chuo-ku, Kumamoto 860-0811, Japan

<sup>c</sup>Department of Biology of the Cell Nucleus, Institute of Molecular Genetics of the Academy of Sciences of the Czech Republic, v.v.i., Vídeňská 1083, 142 20 Prague, Czech Republic

<sup>d</sup>Image Informatics and Computational Biology Unit, Laboratory of Genetics, National Institute on Aging, National Institutes of Health, 251 Bayview Boulevard, Suite 100, Baltimore, MD 21224, USA

<sup>e</sup>Core Research for Evolutional Science and Technology (CREST), Japan Science and Technology Agency, Tokyo 102-0076, Japan

### Abstract

The actin family members, consisting of actin and actin-related proteins (ARPs), are essential components of chromatin remodeling complexes. ARP6, one of the nuclear ARPs, is part of the Snf-2-related CREB-binding protein activator protein (SRCAP) chromatin remodeling complex, which promotes the deposition of the histone variant H2A.Z into the chromatin. In this study, we showed that ARP6 influences the structure and the function of the nucleolus. ARP6 is localized in the central region of the nucleolus, and its knockdown induced a morphological change in the nucleolus. We also found that in the presence of high concentrations of glucose ARP6 contributed to the maintenance of active ribosomal DNA (rDNA) transcription by placing H2A.Z into the chromatin. In contrast, under starvation, ARP6 was required for cell survival through the repression of rDNA transcription independently of H2A.Z. These findings reveal novel pleiotropic roles for the actin family in nuclear organization and metabolic homeostasis.

### Keywords

Actin-related protein; ARP6; Histone H2A.Z; Nucleolus; Wndchrm

---

\*Corresponding author. mharata@biochem.tohoku.ac.jp (M. Harata).

<sup>1</sup>These authors equally contribute to this work.

### Appendix A. Supplementary data

Supplementary data related to this article can be found at <http://dx.doi.org/10.1016/j.bbrc.2015.07.005>.

### Transparency document

Transparency document related to this article can be found online at <http://dx.doi.org/10.1016/j.bbrc.2015.07.005>.

## 1. Introduction

Gene functions are regulated by the modulation of chromatin structure as well as by the spatial association of genes with nuclear regions, including the nuclear lamina and the nucleolus. Chromatin remodeling complexes play central roles in the change of chromatin structure through their enzymatic activity and their regulatory subunits.

The actin family consists of conventional actin and of actin-related proteins (ARPs). The ARPs share the evolutionarily conserved basal structure with actin, which is called the actin fold. In addition, each ARP has individual features. ARPs are classified into ten subfamilies according to the degree of similarity to actin. Among these subfamilies, ARPs 4, 5, 6, 7, 8, and 9 are predominantly localized in the nucleus and were found in chromatin remodeling and histone modification complexes [1]. For example, vertebrate ARP6 is an essential subunit of the Snf-2-related CREB-binding protein activator protein (SRCAP) chromatin remodeling complexes together with  $\beta$ -actin and ARP4 [2,3]. The yeast homolog of the SRCAP complex, the SWR1 chromatin remodeling complex, also includes the same actin family molecules. We have previously shown that nuclear ARPs are indispensable for the function of chromatin remodeling complexes [3]. Particularly, the vertebrate ARP6 is essential for the activity of the SRCAP complex [3]. The SRCAP complex incorporates the histone variant H2A.Z into nucleosomes at promoter regions. H2A.Z plays important roles in epigenetic regulation and chromosome architecture and is associated with a variety of cellular mechanisms, including stem cell maintenance, cellular proliferation, and stress response, through transcriptional regulation and chromosome architecture [4–6].

Nuclear actin family proteins have additional roles in nuclear domain organization independently of the chromatin remodeling complexes. Actin directly interacts with lamins [7], and the dynamics of nuclear actin contribute to nuclear morphology [8,9]. In budding yeast, a fraction of ARP6 is free from the SWR1 complex and regulates genes encoding ribosomal proteins by relocating the gene loci to the nuclear periphery [10]. In addition, vertebrate ARP6 is involved in the spatial organization of chromosome territories in a SRCAP complex-dependent and -independent manner [11].

The nucleolus is composed of three compartments. The fibrillar center (FC) and the dense fibrillar component (DFC) occupy the central region, where ribosomal DNA (rDNA) and pre-ribosomal RNA (pre-rRNA) are transcribed. The granular component (GC) surrounds the FC-DFC component and consists of ribosomal proteins assembled into pre-ribosomes. Ribosomal biogenesis consists of multiple steps, starting from transcription and processing of pre-rRNAs and ending with ribosome assembly. These processes are required for protein synthesis, which consume substantial amounts of cellular energy [12]. Therefore, rDNA transcription and ribosome assembly are linked to cell proliferation [13–16]. Under nutrient shortage, cells preserve cellular energy by downregulating ribosome biosynthesis, thus protecting cells from energy deprivation-induced apoptosis [14,17]. Therefore, the nucleolus supplies sufficient amount of ribosomes for cell growth in the presence of glucose, whereas this activity is switched off upon nutrient deprivation. Although several studies have been performed [14,18], a molecule linking nucleolar organization and function has not been fully investigated.

Here, we analyzed the involvement of vertebrate ARP6 in the organization of the nucleolus and in the transcriptional regulation of rDNA. Loss of function analyses suggested that ARP6 contributes to the morphological organization and functions of the nucleolus. In the presence of high concentrations of glucose, ARP6 maintains rDNA transcription possibly through the incorporation of histone H2A.Z into the chromatin. Instead, upon glucose deprivation, ARP6 contributes to the repression of rDNA transcription to avoid cell death, independently of H2A.Z. From these results, we propose a dual role for ARP6 in rDNA transcription homeostasis, one dependent and the other independent of H2A.Z.

## 2. Materials and methods

### 2.1. Cell culture and treatment

DT40 cells were cultured at 38.5 °C under 5% CO<sub>2</sub> in DMEM (Wako) supplemented with 10% fetal bovine serum, 1% chicken serum, penicillin-streptomycin (Gibco) and 10 μM 2-mercaptoethanol (Wako). HeLa cells were maintained as described previously [19]. For glucose deprivation, DT40 cell pellet was washed twice with 10 mL of phosphate-buffered saline PBS (-) and cultured in DMEM medium without glucose (Gibco), supplemented as described above. For the selective inhibition of the Pol I activity, HeLa cells were treated with actinomycin D (Wako) at 5 nM for 3 h. Dead cells were counted by Trypan blue staining. For RNAi-mediated ARP6 knockdown, HeLa cells were transfected with siRNAs using RNAiMAX (Invitrogen). The cells were analyzed 48 h after transfection. The siRNA duplexes used are: HSS148894 for si*ARP6* (i) and HSS148895 for si*ARP6* (ii) (Invitrogen). The target sequence for the control (siControl) is: CUUACGCUGAGUACUUCGA (GL3, Nippon EGT). To repress the expression of the tetracycline-responsive transgenes in DT40 cells, ARP6 and H2A.Z conditional knockout cell lines (*ARP6*-KO and *H2A.Z*-KO) were treated with tetracycline (Wako) at a final concentration of 2 μg/mL [11]. The cells were analyzed 4–6 days (*ARP6*-KO) and 3–4 days (*H2A.Z*-KO) after the tetracycline treatment, when the proteins were almost absent [11].

### 2.2. Immunofluorescence microscopy

To investigate the subcellular localization of ARP6, immunofluorescence analyses were performed as follows. HeLa cells grown on coverslips were transfected with a Flag-hARP6 cDNA construct [20] using Lipofectamine 2000 (Invitrogen). The cells were fixed with freshly prepared 4% paraformaldehyde/PBS for 15 min at room temperature and then permeabilized with 0.5% Triton X-100 for 10 min. The monoclonal anti-Flag M2 antibody (F1804, Sigma–Aldrich) and polyclonal anti-RPA194 antibody (Santa Cruz) were used for the detection of Flag-hARP6 and RPA194, respectively. Nuclei were visualized with DAPI and the coverslips were mounted with vector shield (Vector Laboratories Inc.). Images were acquired with a confocal laser scanning microscope FV1000 (Olympus). To investigate nucleolar morphology, HeLa cells were analyzed by immunofluorescence as described above using anti-Arp6 (Sigma–Aldrich, A1857), anti-upstream binding factor (UBF) (Santa Cruz, sc-13125), anti-fibrillarin (Santa Cruz, ab4566), and anti-B23 (Santa Cruz, sc-6013-R) antibodies. The images were obtained with an IX-71 microscope (Olympus).

### 2.3. Quantification of nucleolar morphology

To measure differences, we performed supervised machine learning of nucleolar images using pattern recognition software, *wndchrm* (weighted neighbor distance using a computed hierarchy of algorithms representing morphology) ver. 1.31 [21–23]. We trained a machine with 70 nucleolar images for each cell type/class. Nuclear regions were pre-excised from immunofluorescent images to be placed in the center of the area in  $150 \times 150$  pixels using the Image J1 program [24]. Cross-validation tests were automatically repeated for 20 times with 56 training/14 test image data set. The options used for the image analysis were a large feature set of 2873 (–l) and multi-processors (–m). To measure pairwise class dissimilarity, morphological distances were calculated as the euclidean distances ( $d = \sqrt{\sum(A-B)^2}$ ) from the values in class probability matrix obtained from the cross-validations [25].

### 2.4. RNA preparation and reverse transcription–quantitative PCR (RT-qPCR)

RNA from HeLa cells or DT40 cells was extracted with the RNeasy Mini kit (QIAGEN) according to the manufacturer's protocol. The RNA was converted into cDNA by reverse transcriptase using random primers (Applied Biosystems). RT-qPCR was performed with ABI Prism 7300 instrument and SYBR Green PCR Master MIX (Applied Biosystems). Values were normalized against  $\beta$ -actin or glyceraldehyde-3-phosphate dehydrogenase (*GAPDH*) gene expression before calculating relative fold changes. The sequences of the primers used are: human pre-ribosomal RNA (pre-*rRNA*): GAACGGTGGTGTGTCGTTTC and GCGTCTCGTCTCGTCTCACT; human *ARP6* (*hARP6*): ATGACGACCTTAGTGCTGGA and GTGCTGTTTTT-GACCGGAAC; human  $\beta$ -actin: ATCGTCCACCGCAAATGCTTCTA and AGCCATGCCAATCTCATCTTGT; gallus pre-*rRNA*: TCGTCTGTAG-GAGCGAGTGAG and CCTTAGCCCAGGACAGAGC; gallus *GAPDH*: GGTGGTGCTAAGCGTGTTA and CCCTCCACAATGCCAA; human *RPL5*: CACTGGCAATAAAGTTTTGGTG and AACCAGGGAATCGTTTGGT; human *RPL11*: CCGCAAACCTCTGTCTCAACA and TGCCAAAGGATCT-GACAGTG; human *RPL21*: GAGCCGAGATAGCTTCCTGA and CTCCTTCCCATTGGTTCTCA. The primers for gallus pre-*rRNA* were designed according to the database sequence (Genebank: AADN02004142.1 and GenBank: DQ018752.1).

## 3. Results and discussion

### 3.1. Localization of ARP6 in the nucleolus

To analyze the involvement of the nuclear actin family in nuclear organization, we first examined the subnuclear localization of ARP6 in HeLa cells by expressing Flag-tagged human ARP6, which was observed in the nucleoplasm and in the nucleolus where DAPI density was low, (Fig. 1A, white arrows). The nucleolar localization of ARP6 was also confirmed by the detection of endogenous ARP6 with a specific antibody (Fig. 1B). Therefore, we concluded that a part of ARP6 is localized in the nucleolus.

Since ARP6 localizes in the central region of the nucleolus where rDNA is transcribed, we further investigated whether ARP6 was involved in rDNA transcription, a nucleolar function. Immunofluorescence analysis showed that the nucleolar ARP6 (Flag-ARP6) partially colocalized with RPA194, the catalytic subunit of RNA polymerase I (Pol I) (Fig. 2, upper

panels). When Pol I transcription was inhibited with a low dose of actinomycin D, ARP6 relocated from the nucleolus to the nucleolar periphery and formed a unique structure, called nucleolar cap, where RPA194 was accumulated (Fig. 2, lower panels). Since many nucleolar factors that relocate to the nucleolar cap after Pol I inhibition are involved in rDNA transcription [26], ARP6 may also play a role in regulation of rDNA transcription.

### 3.2. ARP6 is involved in morphological organization of the nucleolus

To further test the contribution of ARP6 to the nucleolar structure, we depleted ARP6 in HeLa cells with specific siRNAs and visualized the nucleolus by immunofluorescence using antibodies against UBF, fibrillarin, and B23, all markers of the three sub-nucleolar compartments, FC, DFC and GC, respectively. After 48 h from the transfection of the siRNA, *ARP6* mRNA levels were efficiently reduced (Supplementary Fig. 1). ARP6 depletion changed the structures of both the FC and the DFC, where it localizes. The FC (visualized by UBF) in the ARP6 knockdown cells became more condensed, and DFC (visualized by fibrillarin) became smaller and round (Fig. 3A, Supplementary Figs. 2 and 3). ARP6 depletion also had an effect on GC (visualized by B23), which appeared a ring-like shape (Fig. 3A).

To quantitatively assess nucleolar morphology changes, we used a supervised machine learning algorithm, *wndchrm*, which is useful for image classification and detection of morphological differences [21,22,29]. To train the machine, we created five image libraries: *siARP6* (i), *siARP6* (ii), Act D+, *siControl\_1* and *siControl\_2*, each containing 70 nucleolar immunofluorescence images of UBF (Supplementary Fig. 2). Two control image classes, *siControl\_1* and *siControl\_2*, were intentionally created from the cells that were treated with the same siRNA control; one serves as a reference for image comparison and the other as a negative control, since induces no morphological differences. A positive control class, Act D + contains cells treated with low-dose actinomycin D, a Pol I inhibitor that induces changes in nucleolar morphology [18].

The image classification test among the five classes provided marginal class probabilities, from which we calculated pairwise distances that reflect degree of morphological differences (see Materials and method) [25]. As expected, a comparison between control cells (*siControl\_2* vs *siControl\_1*) showed a low level of morphological differences, while ARP6 knockdown cells (*siControl\_2* vs *siARP6* [i] and *siARP6* [ii]) showed significant difference from control cells (*siControl\_2*), similarly to or more than actinomycin D-treated cells (Act D+) (Fig. 3B). Similar results were obtained with fibrillarin-stained nucleoli, which identify DFC (Supplementary Fig. 3).

Unlike *Arp6* deletion in yeast [10], ARP6 knockdown in mammalian cells had a small or no effect on the expression of ribosomal protein genes (Fig. 3C), suggesting that the nucleoli changed their morphologies without modifying the level of ribosomal proteins. Since the proteins are assembled in the nucleolus and expected to contribute to the nucleolar structure, the effect of ARP6 on the nucleolus can be direct. In summary, ARP6 may influence the formation and/or maintenance of the proper nucleolar structure and function.

### 3.3. ARP6 is required for the maintenance of active rDNA transcription through H2A.Z

To investigate the effect of ARP6 dysfunction in rDNA transcription, we used chicken DT40 cell lines (*ARP6*-KO and *H2A.Z*-KO) where tetracycline was used to suppress *ARP6* and *H2A.Z* gene expression [11]. To test whether ARP6 was involved in rDNA transcription in the presence of high glucose, we quantified the relative level of pre-rRNA in *ARP6*-KO cells by RT-qPCR. The rDNA transcription decreased in the absence of ARP6 (Fig. 4A). A portion of vertebrate ARP6 is an essential component of the SRCAP chromatin remodeling complex [3], which deposits H2A.Z into the chromatin. H2A.Z was previously shown to be incorporated in the rDNA promoter [30]. To test the ARP6 function on rDNA chromatin as a component of the SRCAP, we analyzed rDNA transcription in *H2A.Z*-KO cells [11]. Our RT-qPCR experiment showed that pre-rRNA decreased in *H2A.Z*-KO cells to a similar level as in *ARP6*-KO cells, suggesting that H2A.Z plays a significant role in rDNA chromatin (Fig. 4A). These observations suggested that in a high glucose environment ARP6 is involved in the maintenance of active rDNA transcription through the SRCAP complex.

### 3.4. ARP6 contributes to the repression of rDNA transcription under glucose starvation with a SRCAP complex-independent mechanism

The rDNA transcription is regulated by environmental stresses including limited nutrient availability [18]. Under glucose deprivation, cells reduce the rDNA transcription to save energy derived by glucose metabolism [14,17,31], otherwise the cells go through apoptosis due to lack of energy. To test the contribution of ARP6 and H2A.Z to the repression of rDNA transcription, we measured pre-rRNA synthesis in wild-type, *ARP6*-KO, and *H2A.Z*-KO cells under glucose starvation (Fig. 4B). Whereas glucose starvation for 24 h in wild-type cells reduced rDNA transcription (Fig. 4B, two left bars), in *ARP6*-KO cells rDNA transcription was not repressed (Fig. 4B, *ARP6*-KO). On the other hand, under glucose starvation in *H2A.Z*-KO cells rDNA transcription was repressed to a similar level as in wild-type cells (Fig. 4B, *H2A.Z*-KO and the second bar).

Because pre-rRNA transcription was dysregulated in the absence of ARP6 (Fig. 4A and B), we measured cell viability. *ARP6*-KO cells showed a significantly impaired survival under glucose deprivation (Fig. 4C and D). In contrast, cell death was only slightly increased in *H2A.Z*-KO cells. When the relative increase of dead cells was calculated based on their growth in a high glucose environment, *ARP6*-KO cells, but not *H2A.Z*-KO cells, showed a significantly impaired survival under glucose deprivation (Fig. 4E). Therefore, ARP6 may contribute to the repression of rDNA transcription in a nutrient-limited environment independently of the deposition of H2A.Z by the SRCAP complex.

### 3.5. ARP6 is involved in nucleolar function and organization

In this study, we showed that ARP6 is localized in the nucleolus and is required for its structure and function. Our intensive morphological measurement clearly demonstrated that the FC region of the nucleolus, where rDNA transcription takes place, changed its shape upon ARP6 knockdown. ARP6 has a dual role in the regulation of rDNA transcription. In the presence of high glucose, when cells grow steadily, ARP6 maintains active rDNA transcription through H2A.Z deposition (Fig. 4). Under glucose starvation, ARP6 is required for the repression of rDNA transcription, and this function may be independent of H2A.Z-

deposition. ARP6 plays a structural role for the nucleolus, either directly or through the regulation of rDNA transcription.

Whereas ARP6 deletion in yeasts leads to derepression of genes encoding ribosomal proteins [10], upregulation of ribosomal protein genes was not observed in *ARP6*-knock down HeLa cells in this study (Fig. 3). The discrepancy might be due to the different spatial localization of these genes in the nucleus; in the yeast, ribosomal protein genes are associated with the nuclear pore complex, but in the vertebrate they are not [10], thus suggesting different roles of yeast and vertebrate ARP6 in the regulation of ribosomal protein genes.

Besides the ribosomal roles, the nucleolus functions also as a stress sensor [13,18,32]. Many of the cell stress signal pathways linked to the nucleolus efficiently block rRNA synthesis, stabilize and activate tumor suppressors, and lead to cell cycle arrest [18,33,34]. Perturbation of ribosomal biogenesis or of nucleolar architecture results in the so-called nucleolar stress, which has been implicated in several diseases [35–38]. Since our study suggests that ARP6 could link nucleolar architecture and function, further analyses on ARP6 might contribute to the elucidation of the relationship between the nucleolus and diseases.

## Supplementary Material

Refer to Web version on PubMed Central for supplementary material.

## Acknowledgments

We thank all the members of the laboratory for the discussions. This work was supported by Grants-in-Aid for Scientific Research on Innovative Areas (25116009) (M.H. and N.S.) and the Human Frontier Science Program (RGP0017) (M.H.). H. K. and H. M. thank the Japan Society for the Promotion of Science (JSPS) for Young Scientist Fellowships.

P. H. was supported by Human Frontier in Science program (RGP0017/2013), A. K. by Ministry of Education, Youth and Sports of the Czech Republic (CZ.1.07/2.3.00/30.0050). This publication is supported by the project “BIOCEV – Biotechnology and Biomedicine Centre of the Academy of Sciences and Charles University” (CZ. 1.05/1.1.00/02.0109), from the European Regional Development Fund and with institutional support (RVO68378050).

IGG is supported by the Intramural Research Program of the U.S. National Institutes of Health, National Institute on Aging.

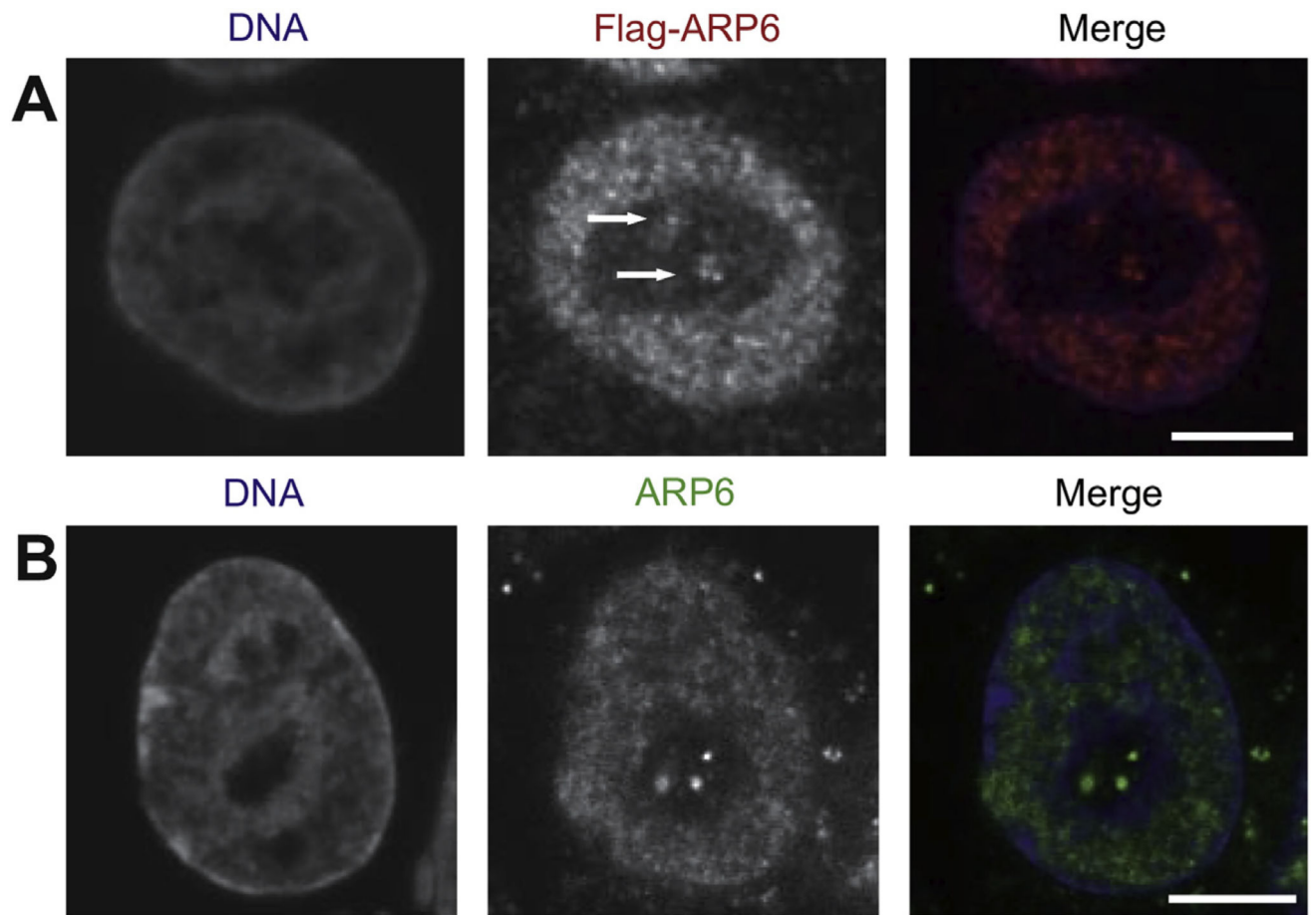
## References

1. Oma Y, Harata M. Actin-related proteins localized in the nucleus: from discovery to novel roles in nuclear organization. *Nucleus*. 2011; 2:38–46. [PubMed: 21647298]
2. Mizuguchi G, Shen X, Landry J, Wu WH, Sen S, Wu C. ATP-driven exchange of histone H2AZ variant catalyzed by SWR1 chromatin remodeling complex. *Science*. 2004; 303:343–348. [PubMed: 14645854]
3. Matsuda R, Hori T, Kitamura H, Takeuchi K, Fukagawa T, Harata M. Identification and characterization of the two isoforms of the vertebrate H2A.Z histone variant. *Nucleic Acids Res*. 2010; 38:4263–4273. [PubMed: 20299344]
4. Kumar SV, Wigge PA. H2A.Z-containing nucleosomes mediate the thermosensory response in *Arabidopsis*. *Cell*. 2010; 140:136–147. [PubMed: 20079334]

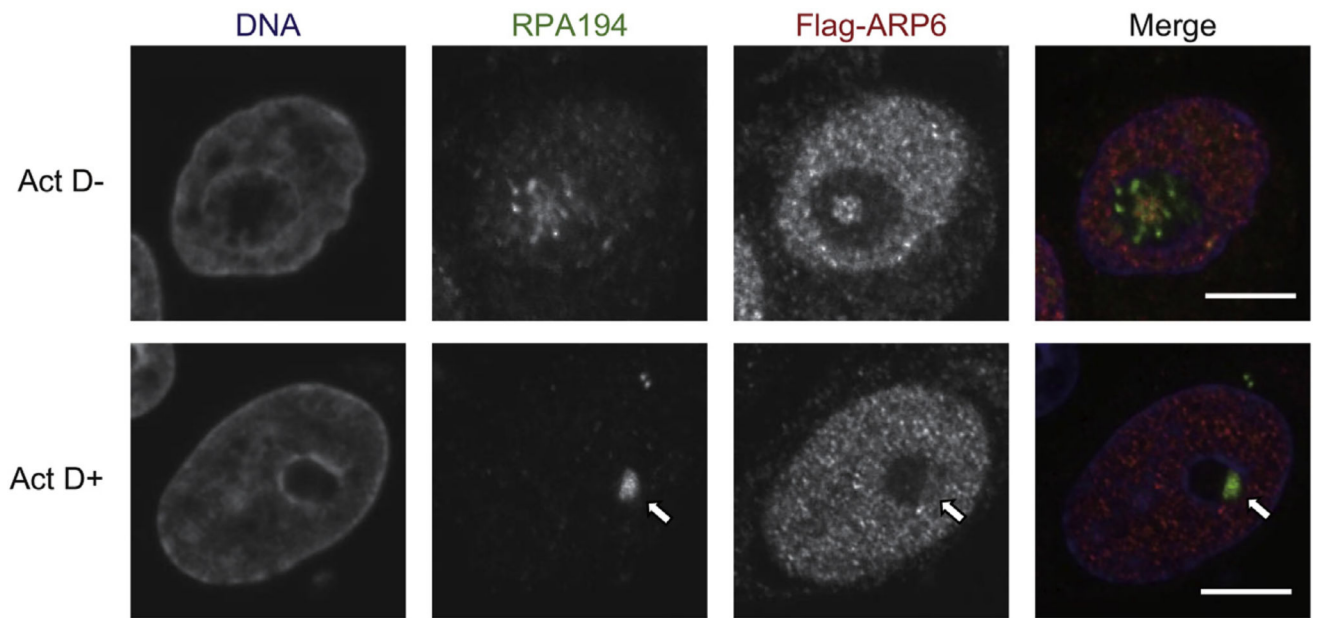
5. Hu G, Cui K, Northrup D, Liu C, Wang C, Tang Q, Ge K, Levens D, Crane-Robinson C, Zhao K. H2A.Z facilitates access of active and repressive complexes to chromatin in embryonic stem cell self-renewal and differentiation. *Cell Stem Cell*. 2013; 12:180–192. [PubMed: 23260488]
6. Gallant-Behm CL, Ramsey MR, Bensard CL, Nojek I, Tran J, Liu M, Ellisen LW, Espinosa JM. DeltaNp63alpha represses anti-proliferative genes via H2A.Z deposition. *Genes Dev*. 2012; 26:2325–2336. [PubMed: 23019126]
7. Simon DN, Zastrow MS, Wilson KL. Direct actin binding to A- and B-type lamin tails and actin filament bundling by the lamin A tail. *Nucleus*. 2010; 1:264–272. [PubMed: 21327074]
8. Cibulka J, Fraiberk M, Forstova J. Nuclear actin and lamins in viral infections. *Viruses*. 2012; 4:325–347. [PubMed: 22590674]
9. Verboon JM, Rincon-Arango H, Werwie TR, Delrow JJ, Scalzo D, Nandakumar V, Groudine M, Parkhurst SM. Wash interacts with lamin and affects global nuclear organization. *Curr. Biol*. 2015; 25:804–810. [PubMed: 25754639]
10. Yoshida T, Shimada K, Oma Y, Kalck V, Akimura K, Taddei A, Iwahashi H, Kugou K, Ohta K, Gasser SM, Harata M. Actin-related protein Arp6 influences H2A.Z-dependent and -independent gene expression and links ribosomal protein genes to nuclear pores. *PLoS Genet*. 2010; 6:e1000910. [PubMed: 20419146]
11. Maruyama EO, Hori T, Tanabe H, Kitamura H, Matsuda R, Tone S, Hozak P, Habermann FA, von Hase J, Cremer C, Fukagawa T, Harata M. The actin family member Arp6 and the histone variant H2A.Z are required for spatial positioning of chromatin in chicken cell nuclei. *J. Cell Sci*. 2012; 125:3739–2743. [PubMed: 22573822]
12. Moss T, Langlois F, Gagnon-Kugler T, Stefanovsky V. A housekeeper with power of attorney: the rRNA genes in ribosome biogenesis. *Cell. Mol. Life Sci*. 2007; 64:29–49. [PubMed: 17171232]
13. Drygin D, Rice WG, Grummt I. The RNA polymerase I transcription machinery: an emerging target for the treatment of cancer. *Annu Rev. Pharmacol. Toxicol*. 2010; 50:131–156. [PubMed: 20055700]
14. Grummt I. The nucleolus-guardian of cellular homeostasis and genome integrity. *Chromosoma*. 2013; 122:487–497. [PubMed: 24022641]
15. Grummt I, Voit R. Linking rDNA transcription to the cellular energy supply. *Cell Cycle*. 2010; 9:225–226. [PubMed: 20023389]
16. Tanaka Y, Okamoto K, Teye K, Umata T, Yamagiwa N, Suto Y, Zhang Y, Tsuneoka M. JmjC enzyme KDM2A is a regulator of rRNA transcription in response to starvation. *EMBO J*. 2010; 29:1510–1522. [PubMed: 20379134]
17. Hoppe S, Bierhoff H, Cado I, Weber A, Tiebe M, Grummt I, Voit R. AMP-activated protein kinase adapts rRNA synthesis to cellular energy supply. *Proc. Natl. Acad. Sci. U. S. A*. 2009; 106:17781–17786. [PubMed: 19815529]
18. Boulon S, Westman BJ, Hutten S, Boisvert FM, Lamond AI. The nucleolus under stress. *Mol. Cell*. 2010; 40:216–227. [PubMed: 20965417]
19. Kitayama K, Kamo M, Oma Y, Matsuda R, Uchida T, Ikura T, Tashiro S, Ohyama T, Winsor B, Harata M. The human actin-related protein hArp5: nucleo-cytoplasmic shuttling and involvement in DNA repair. *Exp. Cell Res*. 2009; 315:206–217. [PubMed: 19014934]
20. Ohfuchi E, Kato M, Sasaki M, Sugimoto K, Oma Y, Harata M. Vertebrate Arp6, a novel nuclear actin-related protein, interacts with heterochromatin protein 1. *Eur. J. Cell. Biol*. 2006; 85:411–421. [PubMed: 16487625]
21. Orlov N, Shamir L, Macura T, Johnston J, Eckley DM, Goldberg IG. WNDCHARM: multi-purpose image classification using compound image transforms. *Pattern Recognit. Lett*. 2008; 29:1684–1693. [PubMed: 18958301]
22. Shamir L, Delaney JD, Orlov N, Eckley DM, Goldberg IG. Pattern recognition software and techniques for biological image analysis. *PLoS Comput. Biol*. 2010; 6:e1000974. [PubMed: 21124870]
23. Eliceiri KW, Berthold MR, Goldberg IG, Ibanez L, Manjunath BS, Martone ME, Murphy RF, Peng H, Plant AL, Roysam B, Stuurman N, Swedlow JR, Tomancak P, Carpenter AE. Biological imaging software tools. *Nat. Methods*. 2012; 9:697–710. [PubMed: 22743775]



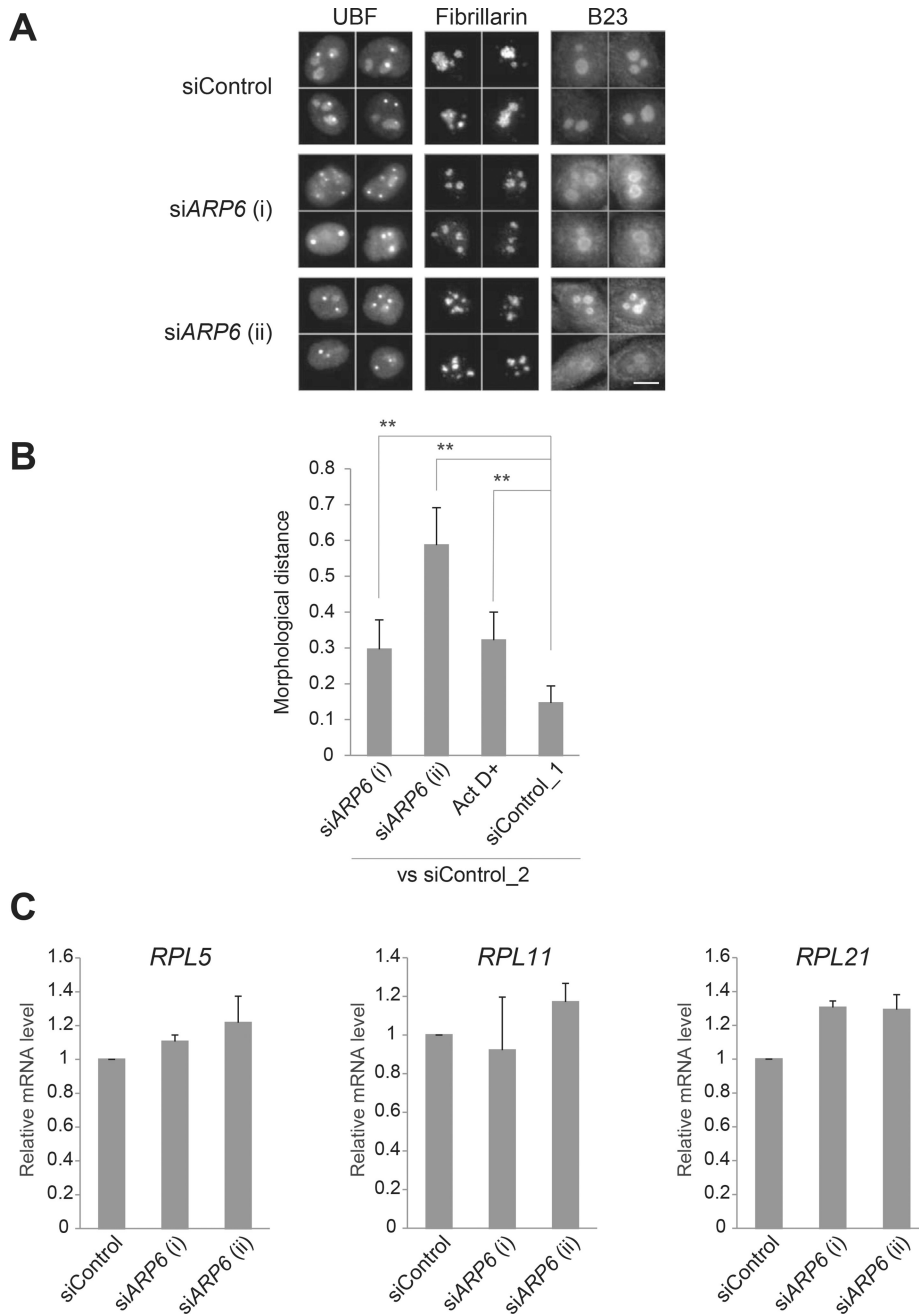
24. Schneider CA, Rasband WS, Eliceiri KW. NIH Image to ImageJ: 25 years of image analysis. *Nat. Methods*. 2012; 9:671–675. [PubMed: 22930834]
25. Johnston J, Iser WB, Chow DK, Goldberg IG, Wolkow CA. Quantitative image analysis reveals distinct structural transitions during aging in *caenorhabditis elegans* tissues. *PLoS One*. 2008; 3:e2821. [PubMed: 18665238]
26. Shav-Tal Y, Blechman J, Darzacq X, Montagna C, Dye BT, Patton JG, Singer RH, Zipori D. Dynamic sorting of nuclear components into distinct nucleolar caps during transcriptional inhibition. *Mol. Biol. Cell*. 2005; 16:2395–2413. [PubMed: 15758027]
29. Shamir L, Orlov N, Eckley DM, Macura T, Johnston J, Goldberg IG. Wndchrm - an open source utility for biological image analysis. *Source Code Biol. Med*. 2008; 3:13. [PubMed: 18611266]
30. van de Nobelen S, Rosa-Garrido M, Leers J, Heath H, Soochit W, Joosen L, Jonkers I, Demmers J, van der Reijden M, Torrano V, Grosveld F, Delgado MD, Renkawitz R, Galjart N, Sleutels F. CTCF regulates the local epigenetic state of ribosomal DNA repeats. *Epigenetics Chromatin*. 2010; 3:19. [PubMed: 21059229]
31. Murayama A, Ohmori K, Fujimura A, Minami H, Yasuzawa-Tanaka K, Kuroda T, Oie S, Daitoku H, Okuwaki M, Nagata K, Fukamizu A, Kimura K, Shimizu T, Yanagisawa J. Epigenetic control of rDNA loci in response to intracellular energy status. *Cell*. 2008; 133:627–639. [PubMed: 18485871]
32. Boisvert FM, van Koningsbruggen S, Navascues J, Lamond AI. The multifunctional nucleolus. *Nat. Rev. Mol. Cell Biol*. 2007; 8:574–585. [PubMed: 17519961]
33. Sloan KE, Bohnsack MT, Watkins NJ. The 5S RNP couples p53 homeostasis to ribosome biogenesis and nucleolar stress. *Cell. Rep*. 2013; 5:237–247. [PubMed: 24120868]
34. Weber JD, Taylor LJ, Roussel MF, Sherr CJ, Bar-Sagi D. Nucleolar Arf sequesters Mdm2 and activates p53. *Nat. Cell Biol*. 1999; 1:20–26. [PubMed: 10559859]
35. Rubbi CP, Milner J. Disruption of the nucleolus mediates stabilization of p53 in response to DNA damage and other stresses. *EMBO J*. 2003; 22:6068–6077. [PubMed: 14609953]
36. Tsai RY, Pederson T. Connecting the nucleolus to the cell cycle and human disease. *FASEB J*. 2014; 28:3290–3296. [PubMed: 24790035]
37. Hetman M. Role of the nucleolus in human diseases. Preface. *Biochim. Biophys. Acta*. 2014; 1842:757. [PubMed: 24631655]
38. Hetman M, Pietrzak M. Emerging roles of the neuronal nucleolus. *Trends Neurosci*. 2012; 35:305–314. [PubMed: 22305768]



**Fig. 1.** Subcellular localization of human ARP6 in HeLa cells. (A) Flag-ARP6 was transiently expressed in HeLa cells and its localization was detected by immunofluorescence with anti-Flag antibodies. ARP6 in the nucleolus is indicated by arrows. (B) Endogenous ARP6 molecules were detected by immunofluorescence using an anti-ARP6 antibody. As in (A), dot-like signals were observed in the nucleolus. Scale bar, 5  $\mu$ m.

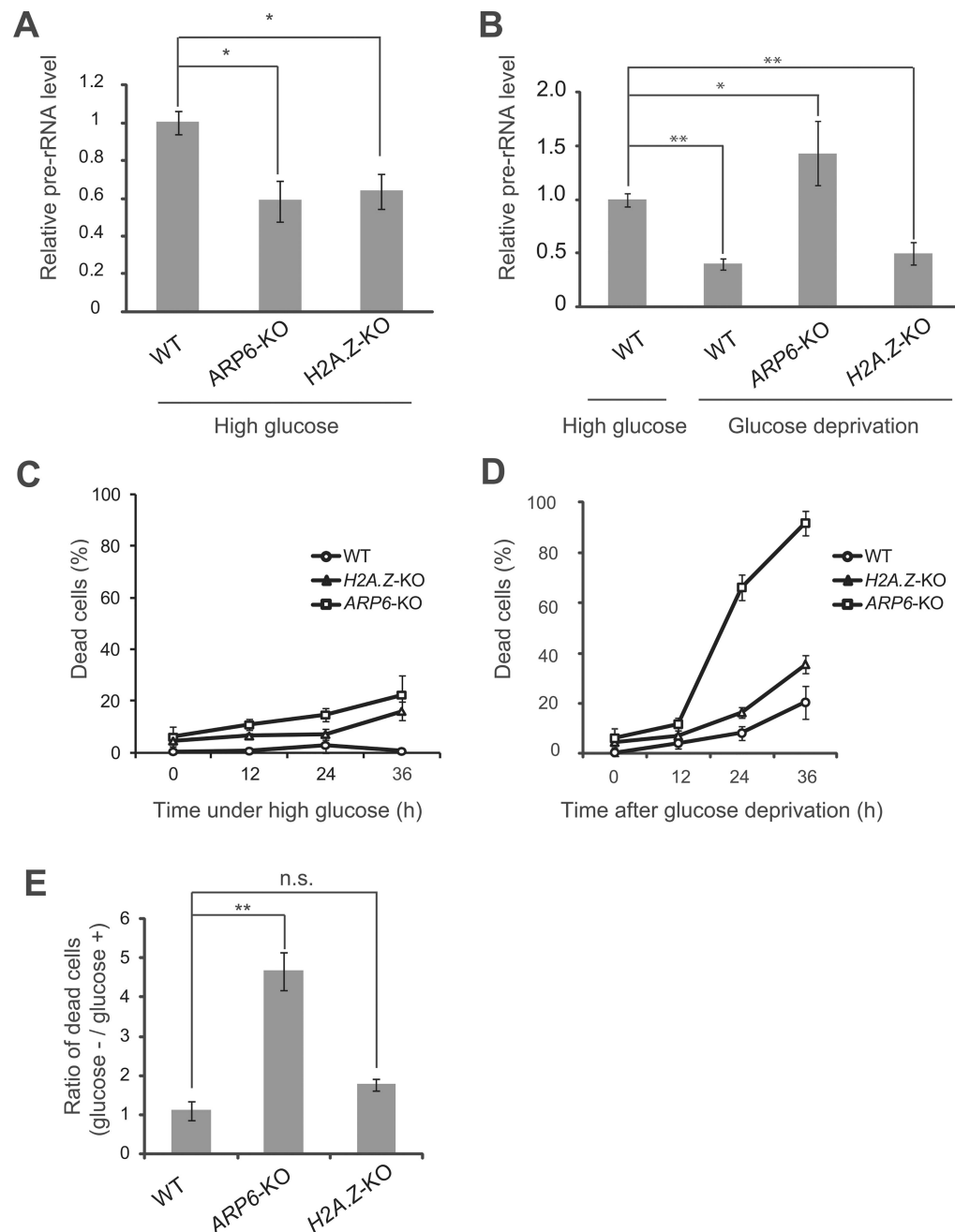


**Fig. 2.** Relocation of ARP6 and RPA194, a catalytic subunit of RNA polymerase I, to the nucleolar cap after the treatment with a low dose of actinomycin D (Act D+). Flag-ARP6 was detected as in Fig. 1A, and RPA194 was detected with a specific antibody. The nucleolar cap by the treatment of actinomycin D was shown by a white arrow. Scale bar, 5  $\mu$ m.



**Fig. 3.** Morphological changes of the nucleolus upon ARP6 depletion. (A) HeLa cells were transfected with siRNA targeting *ARP6* and immunostained with antibodies against UBF, fibrillarin, and B23, specific markers for the nucleolar subcompartments FC, DFC, and GC, respectively. Four representative images for each staining are shown. Scale bar, 10  $\mu$ m. (B) Quantification of morphological difference of the UBF-stained nucleoli was performed with wndchrm, to compute degree of morphological distance from siControl\_2. A large value of the morphological distance indicates that the morphology of the cells is different from the morphology of siControl\_2 cells. siControl\_1 was used as a negative control. Image sets

used in this analysis are shown in Supplementary Fig. 2. Values are means  $\pm$  standard error of 20 cross validation tests; \*\*,  $p < 0.01$ . (C) Ribosomal protein gene expressions in ARP6 knockdown cells. The mRNA was measured with RT-qPCR. *GAPDH* mRNA expression was used as the internal control. Expression levels of control cells are set to 1. Values are represented as means  $\pm$  standard error of triplicates.

**Fig. 4.**

ARP6 is involved in the activation and repression of rDNA transcription. (A) The comparison of rDNA transcription among wild-type (WT), *ARP6*-KO, and *H2A.Z*-KO cells in the presence of high glucose. *GAPDH* was used as the internal control. (B) Analysis of rDNA transcription in WT cells under high glucose (the left bar) and in WT, *ARP6*-KO, and *H2A.Z*-KO cells after glucose deprivation for 24 h (three right bars). *GAPDH* was used as the internal control. (C and D) Cells were cultured with a continuous supply of high-dose glucose (C), or in the absence of glucose (D). Dead cells (%) were counted every 12 h by trypan blue staining. (E) Ratio between dead cells at 24 h after glucose deprivation and cells

under high glucose. For (A), (B) and (E), values represent means  $\pm$  standard error of triplicates; \*,  $p < 0.05$ ; \*\*,  $p < 0.01$ ; n.s. not significant.

Author Manuscript

Author Manuscript

Author Manuscript

Author Manuscript